Polymer 100 (2016) 126–133

Contents lists available at ScienceDirect

Polymer

journal homepage: www.elsevier.com/locate/polymer

Liquid perfluoropolyether electrolytes with enhanced ionic conductivity for lithium battery applications

Kevin R. Olson [a, 2], Dominica H.C. Wong [a, 2, 1], Mahati Chintapalli [b], Ksenia Timachova [c], Rima Janusziewicz [a], William F.M. Daniel [a], Sue Mecham [a], Sergei Sheiko [a], Nitash P. Balsara [c, d, e, **], Joseph M. DeSimone [a, f, *]

[a] Department of Chemistry, University of North Carolina at Chapel Hill, Chapel Hill, NC 27599, United States
[b] Materials Science and Engineering Department, University of California, Berkeley, CA 94720, United States
[c] Department of Chemical Engineering, University of California, Berkeley, CA 94720, United States
[d] Environmental Energy Technologies Division, Lawrence Berkeley National Laboratory, Berkeley, CA 94720, United States
[e] Materials Science Division, Lawrence Berkeley National Laboratory, Berkeley, CA 94720, United States
[f] Department of Chemical and Biomolecular Engineering, North Carolina State University, Raleigh, NC 27695, United States

ARTICLE INFO

Article history:
Received 24 May 2016
Received in revised form
3 August 2016
Accepted 6 August 2016
Available online 8 August 2016

Keywords:
Perfluoropolyether
Electrolyte
Battery

ABSTRACT

We prepared nonflammable liquid polymer electrolytes for lithium-ion batteries by mixing ethoxylated perfluoropolyethers (PFPEs) with $LiN(SO_2CF_3)_2$ salt. Interestingly, we identified the presence of chain coupling in the PFPE polymers and their functionalized derivatives, resulting in a mixture of PFPEs with varying molecular weights. The distribution of molecular weights, along with PFPE's multiple functionalities, allows systematic manipulation of structure to enhance electrochemical and physical properties. Furthermore, the electrolytes exhibited a wide thermal stability window (5% degradation temperature >180 °C). Despite substantial increases in viscosity upon loading the PFPEs with lithium salt, the conductivity ($\sigma \approx 5 \times 10^{-5}$ S cm^{-1} at 28 °C) of the novel electrolytes was about an order of magnitude higher than that of our previously reported PFPE electrolytes. Ethoxylated derivatives of PFPE electrolytes exhibit elevated conductivity compared to non-ethoxylated derivatives, demonstrating our capability to enhance the conductive properties of the PFPE platform by attaching various functional groups to the polymer backbone.

© 2016 Elsevier Ltd. All rights reserved.

1. Introduction

Rechargeable batteries are crucial for accommodating growing energy needs in our society [1,2]. State-of-the-art lithium-ion (Li-ion) batteries are not only incorporated into portable consumer electronic devices and zero-emission vehicles, but also are of interest for electricity storage in smart grid applications [3]. Large-scale use of these batteries has been hindered by the flammability of the electrolyte, which consists of small molecule alkyl carbonates mixed with a lithium salt [4]. Numerous efforts have been made to address this safety concern, including the implementation of cooling systems, external circuitry for disconnecting the battery at high potentials caused by overcharging, and "redox shuttle" molecules for dissipating charge and eliminating thermal runaway [5,6]. However, continual reports of catastrophic battery failures highlight the need for an intrinsically nonflammable Li-ion battery.

Perfluorinated small molecules have been investigated as nonflammable electrolyte alternatives to enhance the safety of Li-ion batteries for potential large-scale applications, but they often exhibit low ionic conductivities due to low lithium salt solubility in the solvent [7]. Therefore, similar to phosphate-based additives, fluorinated small molecules have commonly been explored as flame-retardant additives for conventional alkyl carbonate solvents rather than as neat electrolyte solvents [8]. Although safety

* Corresponding author. Department of Chemistry, University of North Carolina at Chapel Hill, Chapel Hill, NC 27599, United States.
** Corresponding author. Department of Chemical Engineering, University of California, Berkeley, CA 94720, United States.
E-mail addresses: nbalsara@berkeley.edu (N.P. Balsara), desimone@unc.edu (J.M. DeSimone).
[1] Present addresses: Polymers Development Laboratory, Eastman Chemical Company, Kingsport, TN 37660, United States.
[2] These authors contributed equally.

http://dx.doi.org/10.1016/j.polymer.2016.08.020
0032-3861/© 2016 Elsevier Ltd. All rights reserved.

characteristics are enhanced with these additives, the fluorinated solvent often must be the major component in order to observe nonflammability [9,10]. Furthermore, electrolyte-electrode interfacial performance is sacrificed in some cases [11].

Polymer electrolytes have also been investigated as nonflammable electrolytes for Li-ion batteries. Poly(ethylene oxide) (PEO) is by far the most studied polymer electrolyte due to its ability to solvate lithium salts via coordination of ether oxygens to the lithium cation [12–14]. PEO is nonflammable and exhibits high ionic conductivity at elevated temperatures, but it is crystalline at room temperature (melting temperature ≈ 60 °C) [15]. Ion transport occurs via a hopping mechanism in polymer electrolytes, which is closely coupled to segmental motions of the polymer chain. Thus, PEO exhibits room-temperature ionic conductivities that are far below the levels necessary for practical use [15]. In addition, PEO exhibits poor oxidative stability and low Li-ion mobility due to the cation's coordination to backbone oxygens [16,17].

We recently reported that perfluoropolyether (PFPE), a perfluorinated analog of PEO, dissolves the commonly studied salt lithium bis(trifluoromethane)sulfonimide (LiTFSI) and enables the transport of lithium ions [18]. PFPEs are a unique class of fluoropolymers that remain liquids over a wide temperature range [glass transition temperature (T_g) <−80 °C], are nonflammable, and can be chemically tailored to enhance lithium salt solubility.

In addition to the safety enhancement provided by polymer electrolytes and fluorinated solvents, we have proposed that the highly fluorinated PFPE backbone solvates the fluorinated anion of lithium salts, a feature that is distinctive from other polymer and small molecule electrolytes that primarily interact with the lithium cation [8,19–21]. Perfluoroalkyl chains tend to segregate in order to minimize energetically unfavorable interactions between highly nonpolarizable fluorine atoms and other elements [22]. This “fluorous effect” is a powerful tool for molecular adsorption and aggregation in applications such as fluorous solid phase extraction [23], immobilization of biomolecules on microarrays [24], and peptide self-association [25,26], among others. We propose that this fluorous effect causes the PFPE backbone and the highly fluorinated anion of lithium salts to interact significantly.

High transference numbers are achievable in electrolytes that solvate the fluorinated anion of lithium salts, hindering its mobility (rather than that of the Li-ion). Indeed, we previously measured near-unity transference numbers in PFPE/LiTFSI electrolytes, providing evidence that the PFPE backbone solvates the fluorinated anion [18]. However, the conductivity (σ) of the electrolyte—approximately 2.5×10^{-6} S cm^{-1} at 30 °C—must be improved for practical applications, and efforts to accomplish this require establishing the underpinnings of ion transport in the PFPE electrolyte system.

Quantifying the factors that govern ion transport in liquid mixtures is challenging due to the interplay of many factors such as ion solvation, electrostatic coupling, local dynamics in the vicinity of ions, and the glass transition temperature [27–29]. Herein, we report on the synthesis and characterization of a new series of ethoxylated PFPE electrolytes. We elucidate the effect of molecular structure, viscosity, and glass transition temperature on ionic conductivity within the PFPE electrolyte platform.

2. Experimental section

2.1. Materials and sample preparation

Perfluoropolyether Fluorolink E10 was obtained from Solvay-Solexis. Lithium bis(trifluoromethane)sulfonimide (LiTFSI), triethylamine, and methyl chloroformate were obtained from Sigma-Aldrich. 1,1,1,3,3-pentafluorobutane was obtained from MicroCare Corporation. PFPE and LiTFSI were dried at 90 °C under vacuum for at least 24 h prior to use. PFPE and LiTFSI were mixed together and stirred at room temperature for at least 24 h. Salt solubility limits were determined as the point at which the solution visibly changed from transparent to translucent, which has been shown to agree with quantitative measurements (inductively coupled plasma mass spectrometry) for these systems [18].

2.2. Synthesis of DMC-terminated PFPE

Fluorolink E10 (30 g, 0.025 mol) and triethylamine (7 mL, 0.05 mol) were dissolved in 300 mL 1,1,1,3,3-pentafluorobutane at 0 °C under stirring conditions and nitrogen atmosphere. Methyl chloroformate (3.9 mL, 0.05 mol) was added dropwise over 3 min, after which the mixture was heated to 20 °C and stirred for 18 h. The resulting mixture was gravity filtered, washed with water 3×, and washed with brine once. The organic layer was isolated, dried using magnesium sulfate, gravity filtered, and evaporated under reduced pressure. The product was filtered again using a 0.45 micron syringe filter, yielding the final $PFPE_{E10}$-DMC product as a faint yellow, transparent liquid. Yield: 85%. ^{1}H NMR (600 MHz, 25 °C, $(CD_3)_2CO$): 3.54–4.31 ppm (m, 22H). IR (neat): 2885 (C—H), 1751 (C═O), 1183 (C—H), 1067 cm^{-1} (C—O).

2.3. Polymer characterization

Gel permeation chromatography (GPC) measurements were performed on an Agilent Technologies 1260 Infinity LC system equipped with a DAWN HELEOS II multi-angle static light-scattering detector and OptiLab T-rEX refractometer from Wyatt Technologies. The sample (~30 mg/mL in tetrahydrofuran) was eluted through a 3 micron MIXED-E PLgel column (300 mm × 7.5 mm) at 1 mL/min for 60 min. A monodisperse 18 kDa polystyrene sample and monodisperse poly(ethylene glycol) samples of varying molecular weight were used as standards.

A 600 MHz Ultra-Shield Bruker NMR instrument was used for NMR analysis. Quantitative ^{13}C NMRs were obtained by increasing the d1 relaxation delay time until the relative intensity of all peaks remained constant, indicating full relaxation of all carbons. The ^{13}C {^{1}H, ^{19}F} NMR was obtained at a frequency of 150.9028 MHz with relaxation delay d1 = 50 s, 512 scans, ^{1}H decoupling offset = 4 ppm, and ^{19}F decoupling offset = −86 ppm.

2.4. Electrolyte physical properties characterization

Differential scanning calorimetry (DSC) thermograms were recorded using a TA Instruments DSC Q200 on samples that were prepared in air with a temperature range from −150 °C to 100 °C using a heat/cool/heat method at a heating rate of 10 °C/min and cooling rate of 5 °C/min. Glass transition temperatures (T_gs) were determined using the average from the midpoint method on the cooling cycle and second heating cycle thermogram. Thermogravimetric analysis (TGA) was run using a Perkin Elmer Pyris 1 TGA apparatus under nitrogen from 25 °C to 550 °C with a heating rate of 10 °C/min.

An ARES-G2 Rheometer (TA Instruments), equipped with a cone plate (50 mm diameter; 0.0202 radian cone angle), was used to measure viscosity at 25 °C as a function of shear rate, which was ramped from 5×10^{-5} to 50 s^{-1}. The viscosity was modeled using Bingham analysis, which is commonly used to describe viscoplastic materials that exhibit a nonzero shear stress at zero shear rate [30].

2.5. Characterization of ion transport

Electrolyte conductivity was measured in a stainless steel liquid cell using AC impedance spectroscopy. Impedance measurements were performed using a Bio-Logic VMP3 potentiostat, with 20 mV as the input signal amplitude, and 1–10^6 Hz as the frequency range. The minimum in a Nyquist plot of the impedance was used to determine the bulk resistance of the electrolyte, and the geometric factor of the liquid cell, described elsewhere, was used to calculate the conductivity [31]. The temperature of the electrolyte was controlled using a home-built heating chamber. All conductivity measurements were performed in an argon glove box, as the liquid cell was not hermetically sealed.

3. Results and discussion

PFPE is a random copolymer of tetrafluoroethylene oxide and difluoromethylene oxide. Dihydroxyl-terminated Fluorolink D10 (herein, "$PFPE_{D10}$-Diol"), and its ethoxylated Fluorolink E10 analog (herein "$PFPE_{E10}$-Diol") are shown in Fig. 1. Here, $2q$ is the total number of EO repeat units in a single $PFPE_{E10}$ chain, m is the number of tetrafluoroethylene oxide repeat units, and n is the number of difluoromethylene oxide repeat units.

Mass spectrometry indicates that on average, the number of repeat units in a single $PFPE_{E10}$ chain are $q = 2$, $m = 5$, and $n = 4$ (see Fig. S1 in Supporting Information), whereas m and n were previously reported as 7 and 3, respectively, for $PFPE_{D10}$ [18]. We attribute the difference between the m and n values of $PFPE_{E10}$ and $PFPE_{D10}$ to batch-to-batch variation in the industrial synthesis rather than a systematic change between the two analogs.

To our knowledge, there is no precedent for studying a material with perfluoroether, ethylene oxide (EO), and methyl carbonate moieties covalently bound in a single polymer chain. Incorporating all of these functionalities into a pure electrolyte is appealing because EO and methyl carbonate contribute to lithium salt solvation and enhance conductivity [32], while perfluoroether provides thermal stability and high transference of Li-ions [18]. As shown in Scheme 1, $PFPE_{E10}$-Diol (Structure **1**) was functionalized with methyl carbonate endgroups to form DMC-terminated PFPE (herein, "$PFPE_{E10}$-DMC", Structure **2**) in order to enhance electrode-electrolyte compatibility and lithium salt solubility in the polymer. This reaction is analogous to our previously reported functionalization of $PFPE_{D10}$ with DMC endgroups [18].

Chain coupling was unexpectedly observed during the synthesis of $PFPE_{E10}$-DMC from $PFPE_{E10}$-Diol that was not seen with the analogous $PFPE_{D10}$ system. Fig. 2 shows the molecular weight distribution of the PFPE samples, measured using gel permeation chromatography (GPC) in tetrahydrofuran (THF). Each subsequent peak's number-average molecular weight (M_n) was measured to be slightly less than a multiple of the M_n of the first peak, which is consistent with the expected loss of endgroups during chain coupling (peaks at elution time t = 13.3, 13.6, 14.2, and 15.2 min

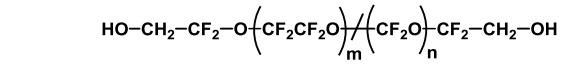

$PFPE_{D10}$-Diol

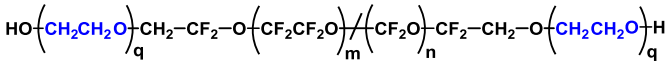

$PFPE_{E10}$-Diol

Fig. 1. Structure of $PFPE_{D10}$-Diol compared to its ethoxylated $PFPE_{E10}$-Diol analog. The slash between the perfluoroether repeat units denotes that it is a random copolymer.

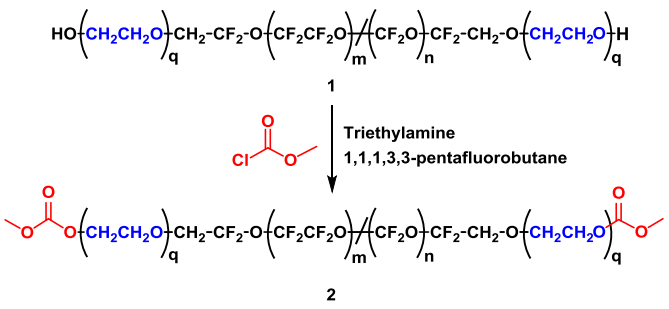

Scheme 1. Synthesis of DMC-terminated $PFPE_{E10}$.

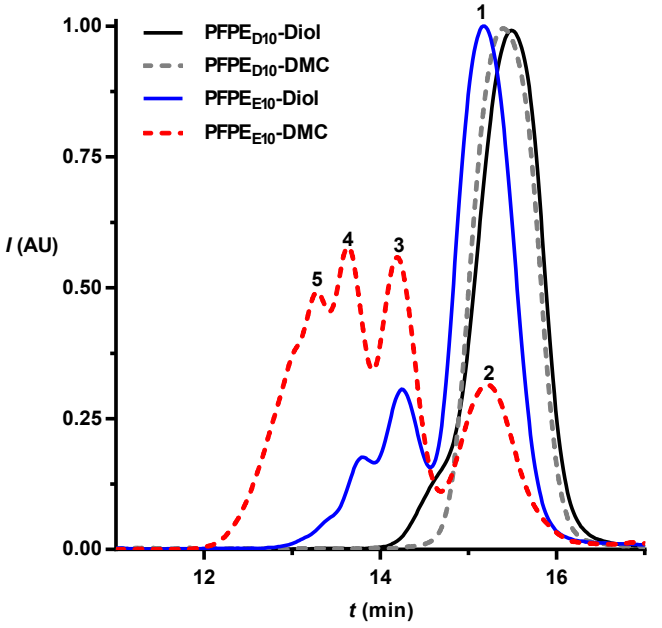

Fig. 2. Comparative GPC chromatograms (light scattering intensity I vs. elution time t) of $PFPE_{E10}$ and $PFPE_{D10}$ oligomers, demonstrating coupling in the E10 derivatives only. The numbers above each peak correspond to the numbered structures shown in Fig. 3.

corresponding to M_n = 5.10, 3.80, 2.60, and 1.46 kDa, respectively, for $PFPE_{E10}$-DMC). Coupling in $PFPE_{E10}$-Diol itself was observed to a lesser extent, while no coupling was observed in $PFPE_{D10}$-Diol and $PFPE_{D10}$-DMC. Therefore, a small degree of coupling occurs during the industrial synthesis of $PFPE_{E10}$-Diol. To our knowledge, this coupling phenomenon in the PFPE Fluorolink E10 has not previously been reported in the literature.

During the addition of DMC endgroups to $PFPE_{E10}$-Diol, we hypothesize that chain coupling increases significantly through the formation of carbonate linkages, as in structures **2**–**5** of Fig. 3. To reject the possibility that ether linkages are formed under our reaction conditions, triethylamine was added to the $PFPE_{E10}$-Diol in the absence of methyl chloroformate. No chain coupling was observed, providing support for the proposed carbonate linkages.

To further support this hypothesis, we used the relative abundance—determined by GPC—of products **2**–**5** and the corresponding number of carbons in each coupled product (assuming carbonate linkages) to calculate the theoretical number of carbons in an average polymer chain (see Table 1 and Fig. S2 in Supporting Information). We then used quantitative ^{13}C NMR spectroscopy and integration methods to determine the relative ratios of terminal methoxy (OCH_3) to carbonyl (C═O) carbons in an average $PFPE_{E10}$-DMC chain. This ratio, as shown in Fig. 4, was determined by NMR

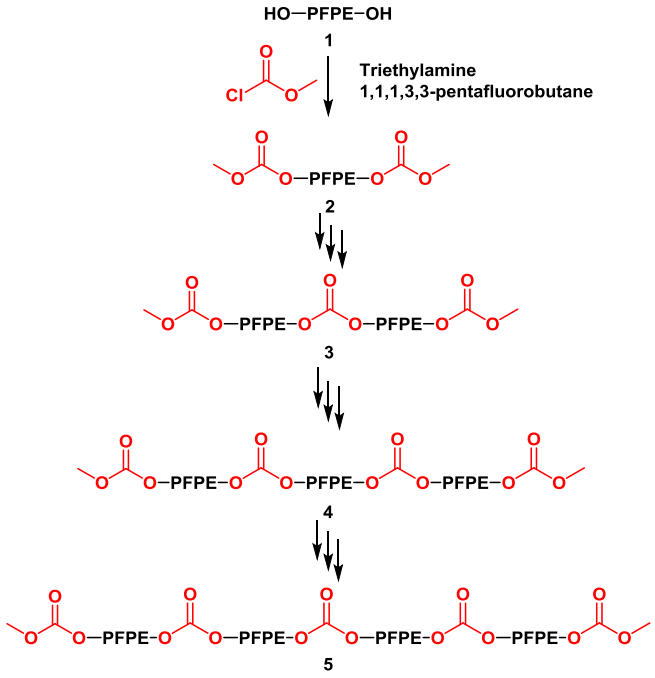

Fig. 3. Proposed structures of coupled products with carbonate linkages. Elution peaks for each numbered compound are shown in Fig. 2.

decomposition temperature of the polymers, represented by the temperature at which 5 wt% of the sample decomposed ($T_{d(5\%)}$). T_gs of the polymers were determined using differential scanning calorimetry (DSC). The $PFPE_{E10}$ polymers are thermally stable ($T_{d(5\%)} > 180\ ^\circ C$) amorphous liquids over a broad temperature range ($T_g < -90\ ^\circ C$). In addition, we found that the presence of lithium salt did not systematically affect the degradation temperature of the PFPE materials.

Increased intermolecular interactions through hydrogen bonding cause $PFPE_{D10}$-Diol to exhibit a higher T_g than $PFPE_{D10}$-DMC. Interestingly, there is little difference in the T_gs of $PFPE_{E10}$-DMC and $PFPE_{E10}$-Diol. Chain coupling in the $PFPE_{E10}$-DMC product, resulting in higher average molecular weight, likely has a competing effect with the reduction in hydrogen bonding on the T_g [37]. The polymers exhibit a similar trend in viscosity (Fig. 5A): in the absence of salt ($r = 0$), hydrogen bonding in $PFPE_{D10}$-Diol leads to higher viscosity than $PFPE_{D10}$-DMC, while chain coupling negates this effect in the $PFPE_{E10}$ polymers.

LiTFSI salt was dissolved in the PFPE polymers to form an electrolyte. The maximum lithium salt-loading in the $PFPE_{E10}$ polymers, as shown in Table 2, was significantly higher than in the $PFPE_{D10}$ polymers (note: r is herein defined as $[Li^+]/[m + n + q]$). This enhanced solubility indicates strong contributions from the EO portions of the backbone to lithium salt solvation, as expected [32,38]. Accordingly, the addition of methyl carbonate endgroups only marginally enhanced lithium salt solubility in the polymer.

Table 1
Abundance and structural differences between coupled products of Fig. 3.

Structure	# of terminal methoxy (OCH_3) C's per chain	# of carbonyl (C=O) C's per chain	Relative abundance (weight fraction)
2	2	2	0.43
3	2	3	0.25
4	2	4	0.05
5	2	5	0.27

to be 2.0:2.9, which is in good agreement with the theoretical integration ratio of 2.0:2.7 based on the GPC results and proposed structures. There are more than two carbonyl carbons per chain, supporting the presence of carbonate linkages. If chain coupling did not occur through carbonate linkages, the only carbonyl groups in the polymer would be endgroups, and the aforementioned ratio would be exactly 2.0:2.0.

Electrolytes consisting of a mixture of distinct molecular weight (MW) polymer chains are rare in the literature, despite Preechatiwong's and Schultz's previous findings that blends of three MWs of poly(ethylene oxide) (PEO) resulted in higher conductivity than a single MW or a blend of two MWs [33]. Very low MW polymer chains remain unentangled and have low viscosities, which enhances conductivity. However, they are too short to behave as random coils and generate significant free volume, which is necessary for ion transport from site to site in amorphous polymer electrolytes [34]. Relatively higher MW polymers (≥5000 g/mol) not only create free volume but also have been proposed by many to allow conducting tunnels to form in PEO [35,36]. Although many polymer electrolytes in the literature are polydisperse, few meet the criterion of containing MWs both above and below the threshold for entanglements, which can potentially provide diverse benefits in an electrolyte. For this reason, we were interested in further investigating our electrolyte composed of a variety of distinct MW PFPE chains.

The physical properties of the PFPE oligomers are compared in Table 2. Thermogravimetric analysis was used to analyze the

The lithium salt solubility in PFPE was lower than in PEO, which dissolves approximately 81 wt% LiTFSI [32], but comparable to the salt concentrations in commercial alkyl carbonate electrolytes, which are typically near 1.0 M [39]. It should be noted that the concentration of dissolved lithium salt in PFPE electrolytes is not directly equivalent to the concentration of charge carriers. Ion pairing occurs in weak, concentrated electrolytes, including polymer electrolytes, and is likely prevalent in this system as well [40]. Ion pair formation results in the presence of uncharged species, reducing the effective concentration of charge carriers contributing to ionic conductivity.

Fig. 5A, B shows the viscosity (η) and T_g of the electrolytes at various salt concentrations. Addition of LiTFSI significantly increased the viscosity and T_g of the $PFPE_{E10}$ electrolytes. This is unsurprising, as complexation with lithium ions forms transient ionic crosslinks, which reduces chain mobility and thus raises viscosity and Tg [41]. It follows that the $PFPE_{D10}$ system experienced only moderate increases in viscosity and T_g because the electron-withdrawing fluorine groups reduce the strength of physical crosslinks between Li-ions and oxygen atoms in the polymer backbone.

In contrast to viscosity and T_g, conductivity at 28 °C in the $PFPE_{E10}$ electrolytes was a non-monotonic function of lithium salt concentration, reaching a maximum at $r = 0.03$, as shown in Fig. 5C. Previous studies have reported the LiTFSI concentration at which PEO electrolytes reach a maximum in conductivity at $r = 0.085$ [32]. In the dilute regime of polymer electrolytes, it is well known that

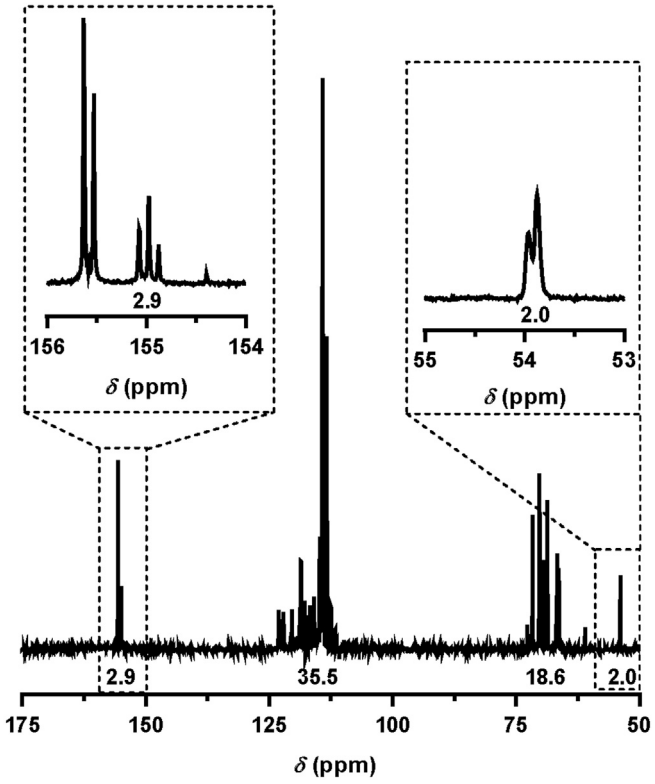

Fig. 4. Quantitative ^{13}C NMR of $PFPE_{E10}$-DMC with corresponding integrations. Inset: carbonyl (δ = 155 ppm) and terminal methoxy (δ = 54 ppm) regions.

Table 2
Physical properties of PFPE polymers.

Electrolyte	$T_{d(5\%)}$ (°C)	T_g (°C)	Maximum [LiTFSI]		
			(wt%)	(mol L^{-1})	(r)
$PFPE_{D10}$-Diol	210	−89	11%	0.76	0.04
$PFPE_{D10}$-DMC	212	−95	19%	1.45	0.09
$PFPE_{E10}$-Diol	181	−93	30%	2.57	0.14
$PFPE_{E10}$-DMC	194	−92	31%	2.70	0.16

conductivity increases upon addition of lithium salt due to elevations in the number of available charge carriers. At higher salt concentrations, addition of lithium salt causes conductivity to decrease because any increase in the number of charge carriers is more than offset by the elevations in T_g and viscosity induced by transient ionic crosslinks, which reduce ion mobility [42]. The behavior of $PFPE_{E10}$ electrolytes spanned both of these regimes. In contrast, conductivity in the $PFPE_{D10}$ electrolytes increased monotonically with salt concentration. We propose that LiTFSI reaches its solubility limit in the $PFPE_{D10}$ polymers before entering the second regime in which elevations in viscosity and T_g overtake the greater number of available charge carriers.

Conductivity was about an order of magnitude higher in the $PFPE_{E10}$ electrolyte than in its $PFPE_{D10}$ analog at 9.1 wt% LiTFSI ($\sigma \approx 5 \times 10^{-5}$ S cm^{-1} and $\sigma \approx 5 \times 10^{-6}$ S cm^{-1}, respectively), despite the elevated viscosity in the former. This observation was unexpected. Considering that transport of ionic species in polymer electrolytes is generally accepted to be closely coupled to segmental motions of polymer chains [43], conductivity typically decreases with increasing viscosity. To further analyze this observation, Fig. 6 shows temperature-dependent conductivity measurements of the PFPE systems at 9.1 wt% LiTFSI.

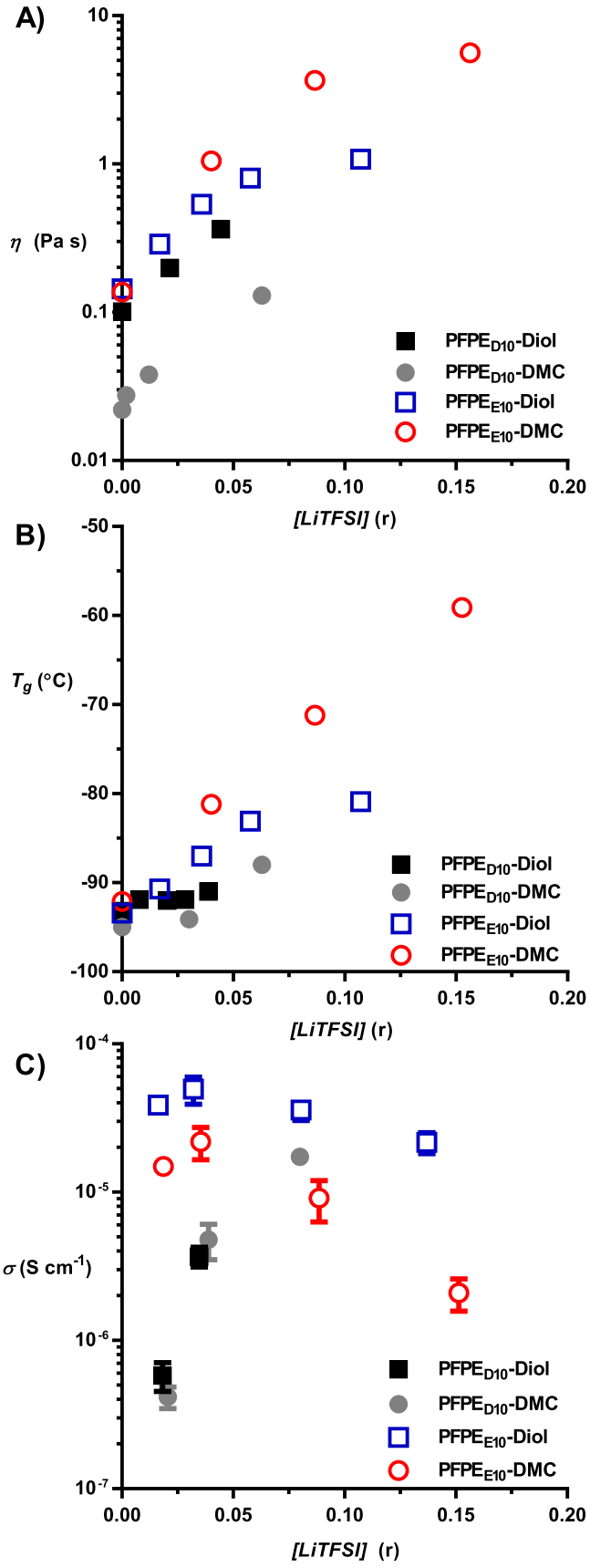

Fig. 5. Effect of LiTFSI salt-loading on A) viscosity at 28 °C, B) glass transition temperature, and C) conductivity at 28 °C.

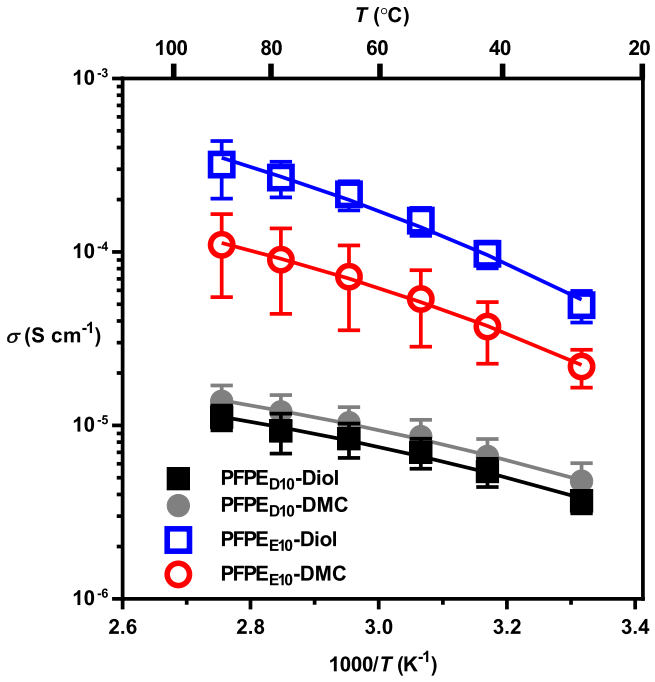

Fig. 6. Conductivity of PFPE electrolytes at 9.1 wt% LiTFSI.

The temperature dependence of the ionic conductivity in the PFPE electrolytes was found to be well described by the Vogel-Fulcher-Tamman (VFT) equation [44–46].

$$\sigma(T) = \frac{A}{\sqrt{T}} \exp\left[\frac{-B}{R(T - T_0)}\right] \quad (1)$$

where σ is the ionic conductivity, A is a constant proportional to the number of charge carriers, B is equivalent to the activation energy for ion transport, R is the gas constant, T is the experimental temperature, and T_0 is an empirical reference temperature (chosen here as T_g−50 K) [47]. Fits to this equation are shown as solid lines in Fig. 4, and the parameters are listed in Table 3.

From the VFT fit parameters, it is clear that in spite of higher activation energies for ion motion, the conductivity of $PFPE_{E10}$ electrolytes is high due to an elevated number of charge carriers (i.e., significantly higher A values in $PFPE_{E10}$ electrolytes). This is consistent with our previous findings that electrolytes based on physical blends of $PFPE_{D10}$/PEG contain significantly more free charge carriers than electrolytes based on $PFPE_{D10}$ alone [48]. Even at the same concentration of dissolved lithium salt (a macroscopic property), the number of mobile charge carriers in $PFPE_{E10}$ electrolytes (a microscopic property) is higher. We attribute this primarily to strong interactions between Li-ions and EO, resulting in enhanced ion solvation. It is also this strong interaction between EO and Li-ions that hinders ion mobility at high salt concentrations in the $PFPE_{E10}$ polymers to a greater extent than in the $PFPE_{D10}$ polymers.

In addition, it has been reported that the dielectric constant of PFPE (without ethylene oxide moieties) ranges between 2.0 and 2.9, while PEO exhibits a dielectric constant approximately double that ($\varepsilon \approx 5$) [49,50]. The presence of hydrogenated ethers likely modestly increases the dielectric constant of $PFPE_{E10}$ compared to $PFPE_{D10}$ and contributes to ion dissociation, although we believe the factors discussed previously—ion solvation and segmental mobility—are primarily responsible for the observed results.

Comparisons between the behavior of $PFPE_{E10}$ and $PFPE_{D10}$/PEG blends demonstrate that unique properties are introduced into the electrolytes by covalently attaching EO to PFPE rather than physically blending the two together. Covalently bonding EO to PFPE eliminates the complex phase interactions between PFPE and PEG in the presence of LiTFSI [48]. It should be noted that the EO content (33 mol% for PFPE/PEG blends and 30 mol% for $PFPE_{E10}$) and lithium salt concentration ($r = 0.026$ for PFPE/PEG and $r = 0.032$ for $PFPE_{E10}$) of both of the investigated electrolytes was comparable.

As we have previously shown [18], the endgroup of the $PFPE_{D10}$ electrolytes did not significantly affect conductivity at a given salt concentration. In contrast, the conductivity of the $PFPE_{E10}$-DMC was appreciably lower than that of $PFPE_{E10}$-Diol. We attribute this to chain coupling in the former, which causes increases in molecular weight along with viscosity and T_g. However, coupling of PFPE chains links EO blocks together, which may introduce a competing effect with viscosity by allowing these salt-loaded blocks to segregate and create conductive channels as has previously been reported for PEO block copolymer-based electrolytes [36].

In short, high charge carrier concentrations in $PFPE_{E10}$ electrolytes overcome the effects of higher glass transition temperatures (compared to $PFPE_{D10}$ electrolytes) on ionic conductivity. Full characterization of the ionic species and concentrations in a weak, concentrated electrolyte system is non-trivial, as many-body ion interactions may be present [51]. Further investigation of ion pairing, including quantitative determination of charge carrier concentrations in PFPE electrolytes, is currently underway. We thoroughly discuss the complex connection between continuum transport properties (e.g., conductivity and transference number) and microscopic transport properties (e.g., ion dissociation and self-diffusivity) in PFPE electrolytes elsewhere [52].

Table 3
VFT fit parameters for PFPE electrolytes at 9.1 wt% LiTFSI.

Electrolyte	A (S cm^{-1} K$^{1/2}$)	B (kJ mol^{-1})	T_0 (K)
$PFPE_{D10}$-Diol	$5.3 \times 10^{-3} \pm 1.7 \times 10^{-3}$	6.0 ± 0.5	134
$PFPE_{D10}$-DMC	$3.7 \times 10^{-3} \pm 1.3 \times 10^{-3}$	5.2 ± 0.1	132
$PFPE_{E10}$-Diol	1.5 ± 0.9	10.0 ± 0.6	135
$PFPE_{E10}$-DMC	$1.2 \times 10^{-1} \pm 0.6 \times 10^{-1}$	7.4 ± 0.3	140

4. Conclusion

We have prepared novel liquid perfluoropolyether polymer electrolytes with EO and methyl carbonate functionalities. We discovered unexpected chain coupling in the commercial $PFPE_{E10}$ material that was augmented by our subsequent functionalization of the chains with methyl carbonate endgroups, resulting in carbonate linkages. PFPE electrolytes are thermally stable and exist as liquids at a broad range of temperatures, affording a wide temperature window of operation. Despite significant increases in T_g and viscosity upon salt-loading, the $PFPE_{E10}$ electrolytes exhibit ionic conductivities that are an order of magnitude higher than that of their lower viscosity $PFPE_{D10}$-based analogs at 9.1 wt% LiTFSI.

Commercial alkyl carbonate electrolytes exhibit $\sigma \approx 10^{-2}$ S/cm at room temperature [53]. Although the lower conductivity of this class of PFPE electrolytes (5×10^{-5} S/cm at room temperature) compared to commercial electrolytes is a disadvantage, the improved safety properties and highly unique anion solvation make them worthy of further investigation. We have established a set of structure-property relationships that we will continue to systematically manipulate to further enhance ion transport in this unique electrolyte platform.

Notes

The authors declare no competing financial interest.

Acknowledgment

This work was supported as part of the Center for Mesoscale Transport Properties, an Energy Frontier Research Center supported by the U.S. Department of Energy, Office of Science, Basic Energy Sciences, under award #DE-SC0012673. The assistance of Marc A. ter Horst and Brandie M. Ehrmann with NMR and MS measurements is also gratefully acknowledged.

Appendix A. Supplementary data

Supplementary data related to this article can be found at http://dx.doi.org/10.1016/j.polymer.2016.08.020.

References

[1] J.M. Tarascon, M. Armand, Issues and challenges facing rechargeable lithium batteries, Nature 414 (2001) 359–367, http://dx.doi.org/10.1038/35104644.
[2] J.B. Goodenough, K.-S. Park, The Li-ion rechargeable battery: a perspective, J. Am. Chem. Soc. 135 (2013) 1167–1176, http://dx.doi.org/10.1021/ja3091438.
[3] F. Cheng, J. Liang, Z. Tao, J. Chen, Functional materials for rechargeable batteries, Adv. Mater 23 (2011) 1695–1715, http://dx.doi.org/10.1002/adma.201003587.
[4] B.K. Mandal, A.K. Padhi, Z. Shi, S. Chakraborty, R. Filler, Thermal runaway inhibitors for lithium battery electrolytes, J. Power Sources 161 (2006) 1341–1345, http://dx.doi.org/10.1016/j.jpowsour.2006.06.008.
[5] E. Berdichevsky, S. Kohn, D. Lyons, Battery pack and method for protecting batteries, US7671565 B2, 2010. http://www.google.com/patents/US7671565 (accessed 11.05.15).
[6] Z. Chen, Y. Qin, K. Amine, Redox shuttles for safer lithium-ion batteries, Electrochim. Acta 54 (2009) 5605–5613, http://dx.doi.org/10.1016/j.electacta.2009.05.017.
[7] M. Ue, Y. Sasaki, Y. Tanaka, M. Morita, in: Nonaqueous Electrolytes with Advances in Solvents, Springer, New York, 2014, pp. 93–165, http://dx.doi.org/10.1007/978-1-4939-0302-3_2.
[8] K. Xu, Nonaqueous liquid electrolytes for lithium-based rechargeable batteries, Chem. Rev. 104 (2004) 4303–4318, http://dx.doi.org/10.1021/cr030203g.
[9] J. Arai, No-flash-point electrolytes applied to amorphous carbon/Li_1+xMn_2O_4 cells for EV use, J. Power Sources 119 (2003) 388–392, http://dx.doi.org/10.1016/S0378-7753(03)00258-1.
[10] K. Sato, I. Yamazaki, S. Okada, J. Yamaki, Mixed solvent electrolytes containing fluorinated carboxylic acid esters to improve the thermal stability of lithium metal anode cells, Solid State Ionics 148 (2002) 463–466, http://dx.doi.org/10.1016/S0167-2738(02)00088-7.
[11] M. Ihara, B.T. Hang, K. Sato, M. Egashira, S. Okada, J.-I. Yamaki, Properties of Carbon Anodes and Thermal Stability in $LiPF_6$ ŌMethyl Difluoroacetate Electrolyte, 2003, http://dx.doi.org/10.1149/1.1614269.
[12] G.S. MacGlashan, Y.G. Andreev, Structure of the polymer electrolyte poly(-ethylene oxide)$_6$: $LiAsF_6$, Nature 398 (1999) 792–794, http://dx.doi.org/10.1039/cc9960002169.
[13] P. Lightfoot, M.A. Mehta, P.G. Bruce, Crystal structure of the polymer electrolyte poly(ethylene oxide)$_3$:$LiCF_3SO_3$, Science 262 (1993) 883–885, http://dx.doi.org/10.1126/science.262.5135.883 (80-.).
[14] Y.G. Andreev, P. Lightfoot, P.G. Bruce, Structure of the polymer electrolyte poly(ethylene oxide)$_3$: $LiN(SO_2CF_3)_2$ determined by powder diffraction using a powerful Monte Carlo approach, Chem. Commun. (1996) 2169, http://dx.doi.org/10.1039/cc9960002169.
[15] C. Berthier, W. Gorecki, M. Minier, M.B. Armand, J.M. Chabagno, P. Rigaud, Microscopic investigation of ionic conductivity in alkali metal salts-poly(ethylene oxide) adducts, Solid State Ionics 11 (1983) 91–95, http://dx.doi.org/10.1016/0167-2738(83)90068-1.
[16] M. Watanabe, A. Nishimoto, Effects of network structures and incorporated salt species on electrochemical properties of polyether-based polymer electrolytes, Solid State Ionics 79 (1995) 306–312, http://dx.doi.org/10.1016/0167-2738(95)00079-L.
[17] J. Evans, C.A. Vincent, P.G. Bruce, Electrochemical measurement of transference numbers in polymer electrolytes, Polym. (Guildf.) 28 (1987) 2324–2328, http://dx.doi.org/10.1016/0032-3861(87)90394-6.
[18] D.H.C. Wong, J.L. Thelen, Y. Fu, D. Devaux, A.A. Pandya, V.S. Battaglia, et al., Nonflammable perfluoropolyether-based electrolytes for lithium batteries, Proc. Natl. Acad. Sci. U. S. A. 111 (2014) 3327–3331, http://dx.doi.org/10.1073/pnas.1314615111.
[19] M.B. Armand, Polymer electrolytes, Annu. Rev. Mater. Sci. 16 (1986) 245–261, http://dx.doi.org/10.1146/annurev.ms.16.080186.001333.
[20] R.J. Blint, Binding of ether and carbonyl oxygens to lithium ion, J. Electrochem. Soc. 142 (1995) 696, http://dx.doi.org/10.1149/1.2048519.
[21] Y. Matsuda, T. Fukushima, H. Hashimoto, R. Arakawa, Solvation of lithium ions in mixed organic electrolyte solutions by electrospray ionization mass spectroscopy, J. Electrochem. Soc. 149 (2002) A1045, http://dx.doi.org/10.1149/1.1489687.
[22] M. Cametti, B. Crousse, P. Metrangolo, R. Milani, G. Resnati, The fluorous effect in biomolecular applications, Chem. Soc. Rev. Chem. Soc. Rev. 41 (2012) 31–42, http://dx.doi.org/10.1039/c1cs15084g.
[23] W. Zhang, D.P. Curran, Synthetic applications of fluorous solid-phase extraction (F-SPE), Tetrahedron 62 (2006) 11837–11865, http://dx.doi.org/10.1016/j.tet.2006.08.051.
[24] A. Kwang-Seuk Ko, Firoz A. Jaipuri, N.L. Pohl, Fluorous-based carbohydrate microarrays, J. Am. Chem. Soc. 127 (2005) 13162–13163, http://dx.doi.org/10.1021/ja054811k.
[25] B.C. Buer, R. de la Salud-Bea, H.M. Al Hashimi, E.N.G. Marsh, Engineering protein stability and specificity using fluorous amino acids: the importance of packing effects, Biochemistry 48 (2009) 10810–10817, http://dx.doi.org/10.1021/bi901481k.
[26] H.-Y. Lee, K.-H. Lee, A. Hashim, M. Al-Hashimi, E. Neil, G. Marsh, Modulating protein structure with fluorous amino acids: increased stability and native-like structure conferred on a 4-Helix bundle protein by hexafluoroleucine, J. Am. Chem. Soc. 128 (2006) 337–343, http://dx.doi.org/10.1021/ja0563410.
[27] D.M. Seo, O. Borodin, D. Balogh, M. O'Connell, Q. Ly, S.-D. Han, et al., Electrolyte solvation and ionic association III. Acetonitrile-Lithium salt mixtures-transport properties, J. Electrochem. Soc. 160 (2013) A1061–A1070, http://dx.doi.org/10.1149/2.018308jes.
[28] M. Kunze, Y. Karatas, H.-D. Wiemhöfer, H. Eckert, M. Schönhoff, Activation of transport and local dynamics in polysiloxane-based salt-in-polymer electrolytes: a multinuclear NMR study, Phys. Chem. Chem. Phys. 12 (2010) 6844–6851, http://dx.doi.org/10.1039/b925840j.
[29] N.A. Stolwijk, C. Heddier, M. Reschke, M. Wiencierz, J. Bokeloh, G. Wilde, Salt-concentration dependence of the glass transition temperature in PEO–NaI and PEO–LiTFSI polymer electrolytes, Macromolecules 46 (2013) 8580–8588, http://dx.doi.org/10.1021/ma401686r.
[30] İ.B. Pehlivan, R. Marsal, G.A. Niklasson, C.G. Granqvist, P. Georén, PEI–LiTFSI electrolytes for electrochromic devices: characterization by differential scanning calorimetry and viscosity measurements, Sol. Energy Mater. Sol. Cells 94 (2010) 2399–2404, http://dx.doi.org/10.1016/j.solmat.2010.08.025.
[31] A.A. Teran, M.H. Tang, S.A. Mullin, N.P. Balsara, Effect of molecular weight on conductivity of polymer electrolytes, Solid State Ionics 203 (2011) 18–21, http://dx.doi.org/10.1016/j.ssi.2011.09.021.
[32] S. Lascaud, M. Perrier, A. Vallee, S. Besner, J. Prud'homme, M. Armand, Phase diagrams and conductivity behavior of poly(ethylene oxide)-molten salt rubbery electrolytes, Macromolecules 27 (1994) 7469–7477, http://dx.doi.org/10.1021/ma00103a034.
[33] W. Preechatiwong, J.M. Schultz, Electrical conductivity of poly(ethylene oxide)—alkali metal salt systems and effects of mixed salts and mixed molecular weights, Polym. (Guildf.) 37 (1996) 5109–5116, http://dx.doi.org/10.1016/0032-3861(96)00332-1.
[34] R.D. Lundberg, F.E. Bailey, R.W. Callard, Interactions of inorganic salts with poly(ethylene oxide), J. Polym. Sci. Part A-1 Polym. Chem. 4 (1966) 1563–1577, http://dx.doi.org/10.1002/pol.1966.150040620.
[35] E. Tsuchida, H. Ohno, K. Tsunemi, N. Kobayashi, Lithium ionic conduction in poly(methacrylic acid)-poly(ethylene oxide) complex containing lithium perchlorate, Solid State Ionics 11 (1983) 227–233, http://dx.doi.org/10.1016/0167-2738(83)90028-0.
[36] R. Yuan, A.A. Teran, I. Gurevitch, S.A. Mullin, N.S. Wanakule, N.P. Balsara, Ionic conductivity of low molecular weight block copolymer electrolytes, Macromolecules 46 (2013) 914–921, http://dx.doi.org/10.1021/ma3024552.
[37] T.G. Fox, P.J. Flory, Second-order transition temperatures and related properties of polystyrene. I. Influence of molecular weight, J. Appl. Phys. 21 (1950) 581, http://dx.doi.org/10.1063/1.1699711.
[38] A. Gandini, J.-F. Le Nest, Solid polymer electrolytes (preparation, characterization, properties), Polym. Mater. Encycl. 10 (1996) 7814.
[39] K. Xu, Electrolytes and interphases in Li-ion batteries and beyond, Chem. Rev. 114 (2014) 11503–11518, http://dx.doi.org/10.1021/cr500003w.
[40] R. Dupon, B.L. Papke, M.A. Ratner, D.H. Whitmore, D.F. Shriver, Influence of ion pairing on cation transport in the polymer electrolytes formed by poly(-ethylene oxide) with sodium tetrafluoroborate and sodium tetrahydroborate, J. Am. Chem. Soc. 104 (1982) 6247–6251, http://dx.doi.org/10.1021/ja00387a014.
[41] J. Sun, G.M. Stone, N.P. Balsara, R.N. Zuckermann, Structure–conductivity relationship for peptoid-based PEO–mimetic polymer electrolytes, Macromolecules 45 (2012) 5151–5156, http://dx.doi.org/10.1021/ma300775b.
[42] G.G. Cameron, M.D. Ingram, Liquid polymer electrolytes, in: J.R. MacCallum, C.A. Vincent (Eds.), Polymer Electrolyte Reviews, Springer, 1989.
[43] M. Marzantowicz, J.R. Dygas, F. Krok, Z. Florjańczyk, E. Zygadło-Monikowska, Influence of crystalline complexes on electrical properties of PEO: LiTFSI electrolyte, Electrochim. Acta 53 (2007) 1518–1526, http://dx.doi.org/10.1016/j.electacta.2007.03.032.
[44] H. Vogel, The law of the relation between the viscosity of liquids and the temperature, Phys. Z. 22 (1921) 645–646.
[45] G.S. Fulcher, Analysis of recent measurements of the viscosity of glasses, J. Am. Ceram. Soc. 8 (1925) 339–355, http://dx.doi.org/10.1111/j.1151-2916.1925.tb16731.x.
[46] G. Tammann, W. Hesse, Die Abhangigkeit der Viscositat von der temperatur bie unterkuhlten Flussigkeiten, Z. Fur Anorg. Und Allg. Chem. 156 (1926) 245–257, http://dx.doi.org/10.1002/zaac.19261560121.
[47] K.P. Barteau, M. Wolffs, N.A. Lynd, G.H. Fredrickson, E.J. Kramer, C.J. Hawker,

Allyl glycidyl ether-based polymer electrolytes for room temperature lithium batteries, Macromolecules 46 (2013) 8988–8994, http://dx.doi.org/10.1021/ma401267w.
[48] D.H.C. Wong, A. Vitale, D. Devaux, A. Taylor, A.A. Pandya, D.T. Hallinan, et al., Phase behavior and electrochemical characterization of blends of perfluoropolyether, poly(ethylene glycol), and a lithium salt, Chem. Mater 27 (2015) 597–603, http://dx.doi.org/10.1021/cm504228a.
[49] G. Marchionni, G. Ajroldi, G. Pezzin, Structure–Property relationships in perfluoropolyethers: a family of polymeric oils, in: Comprehensive Polymer Science Supplement, 1989, pp. 347–388, http://dx.doi.org/10.1016/B978-0-08-096701-1.00248-2.
[50] C. Tonelli, P. Gavezotti, E. Strepparola, Linear perfluoropolyether difunctional oligomers: chemistry, properties and applications, J. Fluor. Chem. 95 (1999) 51–70, http://dx.doi.org/10.1016/S0022-1139(98)00298-X.
[51] W. Wieczorek, D. Raducha, A. Zalewska, J.R. Stevens, Effect of salt concentration on the conductivity of PEO-based composite polymeric electrolytes, J. Phys. Chem. B 102 (1998) 8725–8731, http://dx.doi.org/10.1021/jp982403f.
[52] M. Chintapalli, K. Timachova, K.R. Olson, S.J. Mecham, D. Devaux, J.M. DeSimone, et al., Relationship between conductivity, ion diffusion, and transference number in perfluoropolyether electrolytes, Macromolecules 49 (2016) 3508–3515, http://dx.doi.org/10.1021/acs.macromol.6b00412.
[53] M. Dahbi, F. Ghamouss, F. Tran-Van, D. Lemordant, M. Anouti, Comparative study of EC/DMC LiTFSI and LiPF6 electrolytes for electrochemical storage, J. Power Sources 196 (2011) 9743–9750, http://dx.doi.org/10.1016/j.jpowsour.2011.07.071.